Electronic transitions in CePd$_2$Si$_2$ studied by resonant x-ray emission spectroscopy at high pressures and low temperatures

Hitoshi Yamaoka,[1] Yumiko Zekko,[2] Akio Kotani,[1,3] Ignace Jarrige,[4] Naohito Tsujii,[5] Jung-Fu Lin,[6] Jun'ichiro Mizuki,[2]
Hideki Abe,[5] Hideaki Kitazawa,[5] Nozomu Hiraoka,[7] Hirofumi Ishii,[7] and Ku-Ding Tsuei[7]

[1]*Harima Institute, RIKEN (The Institute of Physical and Chemical Research), Sayo, Hyogo 679-5148, Japan*
[2]*Graduate School of Science and Technology, Kwansei Gakuin University, Sanda, Hyogo 669-1337, Japan*
[3]*Photon Factory, Institute of Materials Structure Science, High Energy Accelerator Research Organization,
1-1 Oho, Tsukuba, Ibaraki 305-0801, Japan*
[4]*National Synchrotron Light Source II, Brookhaven National Laboratory, Upton, New York 11973, USA*
[5]*Quantum Beam Center, National Institute for Materials Science, 1-2-1 Sengen, Tsukuba 305-0047, Japan*
[6]*Department of Geological Sciences, The University of Texas at Austin, Austin, Texas 78712, USA*
[7]*National Synchrotron Radiation Research Center, Hsinchu 30076, Taiwan*

Temperature and pressure dependences of the electronic structure of the heavy-fermion system CePd$_2$Si$_2$ have been investigated using partial fluorescence yield x-ray absorption spectroscopy and resonant x-ray emission spectroscopy at the Ce L_3 edge. The temperature dependence has also been measured for CeRh$_2$Si$_2$ for comparison. In both compounds Ce is in a weakly mixed valence state at ambient pressure, mostly f^1 with a small contribution from the f^0 component. No temperature dependence of the Ce valence is observed at temperatures as low as 8 K. In CePd$_2$Si$_2$ at 19 K, however, the Ce valence shows a continuous increase with pressure, indicating pressure-induced delocalization of the $4f$ states. Theoretical calculations based on the single impurity Anderson model reproduce the experimental results well. Pressure dependence of the difference between the ground state valence and the measured valence including the final state effect is also discussed.

I. INTRODUCTION

Tetragonal Ce-122 compounds such as CeM_2X_2 (M: transition metal; X: Si, Ge) cover a wide range of the Doniach phase diagram, in which the Kondo effect and the Ruderman-Kittel-Kasuya-Yoshida (RKKY) interaction compete with each other and give rise to an interesting variety of ground states.[1] The former screens the local magnetic spin due to the c-f hybridization forming a Kondo singlet ground state, whereas the latter leads to a magnetic order, where c is conduction band. Some of the Ce-122 systems have been observed to exhibit anomalous physical properties, including superconductivity, in the vicinity of the quantum critical point (QCP).[2] A universal Doniach phase diagram based on the calculations for the Kondo lattice model may be applicable for a Ce-122 system. For instance, CeRh$_2$Si$_2$ may be close to the maximum in the Doniach phase diagram and not far from the QCP, whereas CeCu$_2$Si$_2$ is even closer to the QCP. CePd$_2$Si$_2$ is in the regime where the RKKY interaction and the Kondo effect are weak. CeRu$_2$Si$_2$ is in the nonmagnetic Kondo regime where the Fermi liquid state is observed. A universal Doniach phase diagram was proposed for Ce-122 systems based on calculations for the Kondo lattice model.[3]

In this paper, we report experimental results on the electronic structure of CePd$_2$Si$_2$ at high pressures and low temperatures. Temperature dependence of that for CeRh$_2$Si$_2$ has been also measured. Both compounds are known to show pressure-induced superconductivity.[4–6] CePd$_2$Si$_2$ is antiferromagnetic below 10 K at ambient pressure. Extrapolation of the Néel temperature (T_N) to zero yields a pressure of about 2.8 GPa.[7] At 2.8 GPa, above which non-Fermi liquid behavior was observed in the resistivity measurement, showing

a power law of $T^{1.2-1.3}$.[7] The effective paramagnetic moment was $2.61\mu_B$ at ambient pressure,[8] which is close to the calculated value of $2.54\mu_B$ for Ce^{3+}. The Kondo temperature (T_K) was estimated to be 10 K, which is comparable to T_N. The electronic specific coefficient (γ) is 160 mJ mol^{-1}K^{-2},[9] indicating that this system is a heavy fermion superconductor. Superconductivity was observed below 0.3 K in a relatively small pressure window of about ±1 GPa centered at $\sim$2.6 GPa.[7] A broader superconducting pressure range of 2–7 GPa has been reported for a polycrystalline sample.[10]

The Néel temperature in CeRh$_2$Si$_2$ terminates at the onset of superconductivity below 0.5 K over a very narrow pressure range between 1.03 GPa and 1.08 GPa.[5,6] The signature of a further magnetic phase transition, denoted as T_{N_2}, was also indicated.[8] The magnetic moment is $1.42\mu_B$ for Ce at the corner site and $1.34\mu_B$ for Ce at the body-centered site.[11] The effective paramagnetic moment is $2.58\mu_B$,[8] very close to the value for CePd$_2$Si$_2$. γ is 23 mJ mol^{-1}K^{-2}. Nuclear magnetic resonance (NMR) study suggested a relatively high T_K of $\sim$100 K.[8] Interestingly, the Fermi liquid nature is maintained up to 1.28 GPa.[6]

Full potential *ab initio* calculations for CeMSi$_2$ (M = Pd, Rh, Ru) showed a shift in the $4d$ band center toward the Fermi level when the transition metal M is changed from Pd to Ru, indicating that the c-f hybridization is stronger in this order.[12] Spectral properties and the crystal electric field (CEF) splitting effect were further studied using the same theoretical method, showing T_K(CeRh$_2$Si$_2$) > T_K(CeRu$_2$Si$_2$) > T_K(CePd$_2$Si$_2$).[13]

In our study, we employed partial fluorescence yield x-ray absorption spectroscopy (PFY-XAS) and complementary resonant x-ray emission spectroscopy (RXES), which is sensitive

TABLE I. Representative physical properties of Ce-122 compounds. μ_{eff}, Θ, γ, T_{K}, T_{N}, T_{C}, P_{C}, CEF, and v_R are effective paramagnetic moment, Curie-Weiss temperature, electronic specific coefficient, Kondo temperature, Néel temperature, superconducting transition temperature, pressure at maximum T_{C}, crystal electric fields, and spectral weight ratio (see the text), respectively. Ce valences are derived from the fit to the PFY-XAS spectra. Note that for $CeRh_2Si_2$ $T_{\mathrm{N1}} = 25$ K and $T_{\mathrm{N2}} = 37$ K.

	μ_{eff} (μ_{B})	Θ (K)	γ (mJ mol^{-1}K^{-2})	T_{K} (K)	T_{N} (K)	T_{C} (K)	P_{C} (GPa)	CEF (K)	v_R
$CePd_2Si_2$	2.61[a]	−75[b]	160[c]	10[b]	10[b]	0.5[d]	2.6[d]	214[h], 220[d,e], 350[f]	3.00 ± 0.01
$CeRh_2Si_2$	2.58[a], 3.0[g]		23[h]	33[b], ∼100[a]	25[c], 37[c]	0.35[i]	0.9[f]	310[g,e]	3.01 ± 0.01

[a]Reference 8.
[b]Reference 16.
[c]Reference 9.
[d]Reference 7.
[e]Reference 13.
[f]Reference 17.
[g]Reference 18.
[h]Reference 6.
[i]Reference 5.

to bulk properties of the samples, to investigate the valence of the Ce ions as a function of temperature and pressure for $CePd_2Si_2$ and as a function of temperature for $CeRh_2Si_2$. We note that a detailed examination of the temperature and pressure dependences of the electronic structures for these compounds had not been performed to date. Our high-pressure results for $CePd_2Si_2$ show a clear pressure-induced change in the electronic structure from the localized $4f$ state to the hybridized itinerant state. We compare the experimental results with theoretical calculations based on the single impurity Anderson model (SIAM). The effects of the final state on the spectra are also discussed in detail.

II. EXPERIMENTS

Single-crystalline samples of $CePd_2Si_2$ and $CeRh_2Si_2$ were grown by the Czochralsky pulling method using a tetra-arc furnace under Ar atomosphere, and were annealed at 800 °C for 1 week under high vacuum.[14] Both samples feature tetragonal $ThCr_2Si_2$-type crystal structure (space group $I4/mmm$, No. 139) with Ce, Pd/Rh, and Si located in the 2a, 4d, and 4e sites, respectively.[15] Physical properties of these compounds are summarized in Table I. $CePd_2Ge_2$ is included for comparison. PFY-XAS and RXES measurements were performed at the Taiwan beamline BL12XU, SPring-8.[19] The undulator beam was monochromatized by a cryogenically cooled double crystal monochromator. Incident photon energies were calibrated by using metal K-absorption edges of V and Cr. The incident photon flux was estimated to be $(7–8) \times 10^{11}$ photons/s at 5.46 keV. A Johann-type spectrometer equipped with a spherically bent Si(400) crystal (a radius of about 1 m) was used to analyze the Ce $L\alpha_1$ ($3d_{5/2} \rightarrow 2p_{3/2}$) and x-ray Raman emission lines around Ce L_3 absorption edge with a solid Si state detector (Amptech). The overall energy resolution was estimated to be 1.5 eV around the emitted photon energy of 4.8 keV. The intensities of the measured spectra were normalized using the incident beam that was monitored just before the sample. A membrane-controlled DAC was used for high pressure experiments at low temperature. A closed-circuit He cryostat was used to achieve temperatures as low as 8 K. For

high-pressure experiments the x-ray beam was focused to a size of 23 (horizontal) × 25 (vertical) μm^2 at the sample position using a toroidal and K-B mirrors. High-pressure conditions were realized using a diamond anvil cell (DAC) with a Be
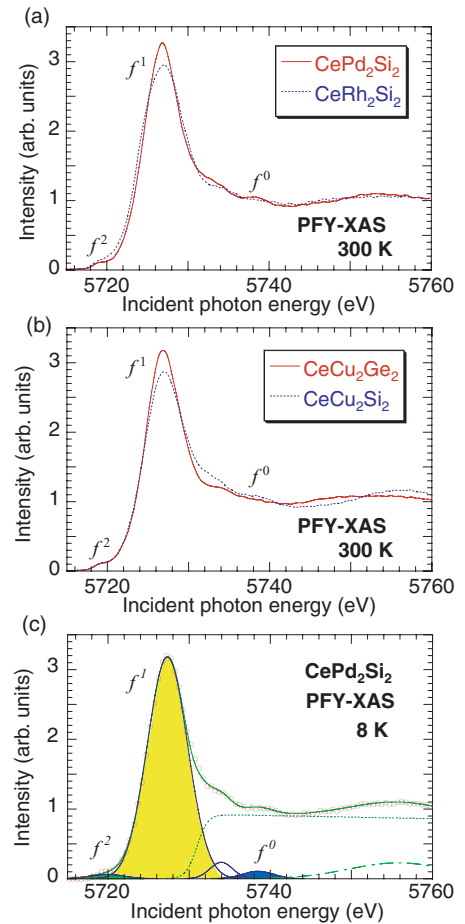

FIG. 1. (Color online) Comparison of the PFY-XAS spectra at 300 K for (a) $CePd_2Si_2$ and $CeRh_2Si_2$ and (b) $CeCu_2Si_2$ and $CeCu_2Ge_2$. (c) An example of the fit to the PFY-XAS spectra (open circles) measured at 8 K for $CePd_2Si_2$.

gasket. 4 : 1 methanol-ethanol mixture was loaded into the sample chamber as the pressure medium. We used the in-plane geometry where both the incoming and outgoing beams passed through the 2-mm-diameter Be gasket with a scattering angle of 90°. The Be gasket was preindented to 38 μm thick and a 180 μm sample chamber was drilled. Pressure was monitored using ruby fluorescence, which is calibrated with an empirical formula[20,21] at low temperature.

III. EXPERIMENTAL RESULTS

A. PFY-XAS

PFY-XAS spectra at 300 K for CePd$_2$Si$_2$ and CeRh$_2$Si$_2$ are shown in Fig. 1. CeCu$_2$Si$_2$ and CeCu$_2$Ge$_2$ are included for comparison. The intensity is normalized to the spectral area. These spectra show that the Ce-122 systems exhibit weak valence fluctuations and mainly consist of f^1 (Ce^{3+}) with small fractions of f^2 (Ce^{2+}) and f^0 (Ce^{4+}). The electronic structures of CePd$_2$Si$_2$ and CeRh$_2$Si$_2$ resemble the relationship between CeCu$_2$Ge$_2$ and CeCu$_2$Si$_2$, as the c-f hybridization and the Kondo temperature of the former are smaller than that of the latter.

In these measurements, we observed a Ce $3d_{5/2} \rightarrow 2p_{3/2}$ deexcitation following a $2p_{3/2} \rightarrow 5d$ excitation. Thus the final state includes a $3d$ core hole, which can cause a dynamical screening effect by the core-hole potential in the final excited state.[22,23] A charge transfer between the ligand and the excited atom can occur; that is, the measured spectra do not necessarily correspond to the ground state. The final-state effect in Ce compounds mainly results in an increase of the f^2 component, while changes in the hybridization affect the ratio between the f^0 and f^1 components. Here
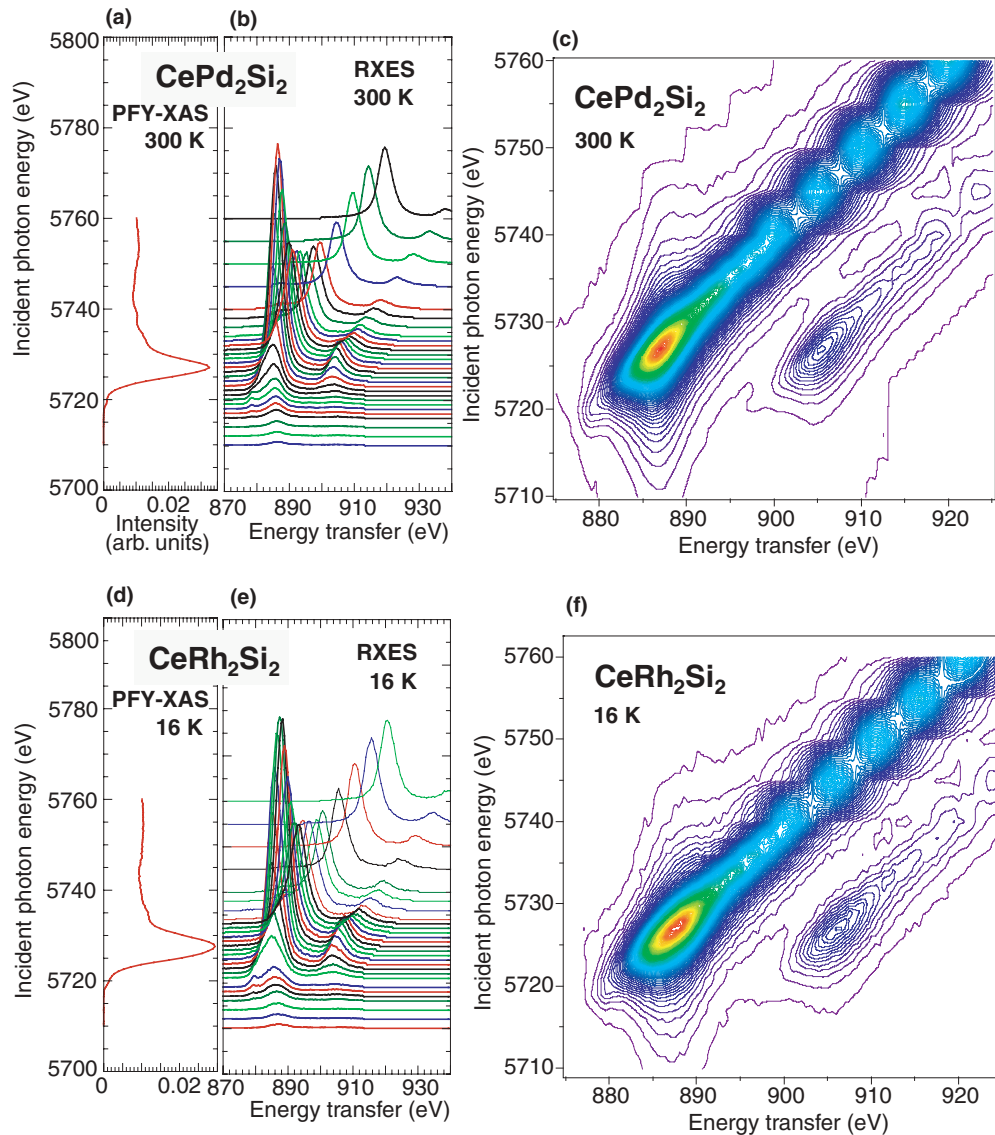

FIG. 2. (Color online) PFY-XAS spectrum (a),(d) with the corresponding $2p$-$3d$ RXES spectra (b),(e) as a function of the incident photon energies for CePd$_2$Si$_2$ at 300 K and for CeRh$_2$Si$_2$ at 16 K. Vertical offset of the RXES spectra in the panel (b),(e) has been scaled to the incident energy axis of the PFY-XAS spectra in the panels (a),(d). Contour images of the RXES spectra are shown in (c) and (f). Spotty structures are an artifact due to the lack of the data between the measured points.

we define the spectral weight ratio (v_R), which correlates with the mean valence in the ground state (v_g), as $v_R = 3 + \{I(f^0) - I(f^2)\}/\{I(f^0) + I(f^1) + I(f^2)\}$, where $I(f^n)$ is the intensity of the f^n component.

Figure 1(c) shows an example of the fit with Voigt functions for the PFY-XAS spectrum of $CePd_2Si_2$ at 8 K. A better fit would require an additional peak at approximately 5733 eV between the modeled f^1 and f^0 peaks. At present, the origin of this peak remains unclear and merits further study. At 300 K v_R is estimated to be 3.00 for $CePd_2Si_2$, 3.01 for $CeRh_2Si_2$, 3.02 for $CeCu_2Si_2$, and 2.99 for $CeCu_2Ge_2$. The error for v_R is on the order of 0.01. The v_R value of $CePd_2Si_2$ is slightly lower than that of $CeRh_2Si_2$, corresponding to a higher T_K for $CeRh_2Si_2$.

B. RXES

Figure 2 shows $2p$-$3d$ RXES spectra as a function of the incident photon energy across the L_3 edge, (b) for $CePd_2Si_2$ at 300 K and (e) for $CeRh_2Si_2$ at 16 K. Energy transfer is
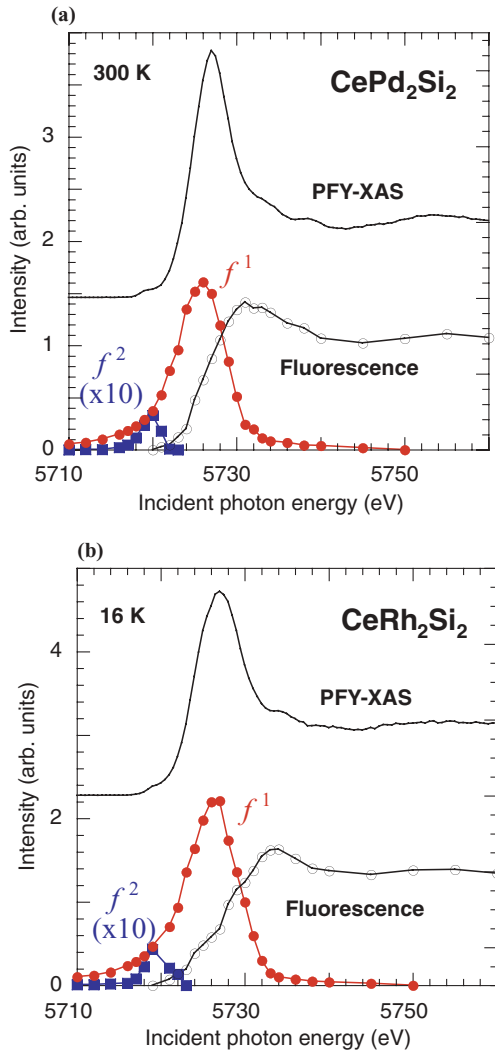

FIG. 3. (Color online) Incident energy dependence of the intensity of the 2+ and 3+ Raman and fluorescence components inferred from the fit of the RXES spectra with the PFY-XAS spectra. The intensity of f^2 component is multiplied by a factor of 10.

defined as the energy difference between the incident and emitted photon energies. We clearly observed double peaks in the x-ray Raman spectra below the absorption edge at ~5723 eV, corresponding to the Ce f^2 and f^1 components with constant transferred energies. Above the absorption edge, the energy transfer of the fluorescence peaks changes linearly with the incident energy. These trends are most visible in the contour maps in Figs. 2(c) and 2(f). We fitted the RXES spectra with Voigt functions using a three-component model including f^2, f^1, and fluorescence components. We note that because of the overlap of the f^0 component with the intense fluorescence component, it is rather difficult to extract the weak f^0 component, which has therefore been neglected. Our modeled results in Fig. 3 confirm the presence of two Raman components with the fluorescence component. The estimated v_R from Fig. 3(a) is 2.99 ± 0.01 for $CePd_2Si_2$, which is is similar to that for $CeRh_2Si_2$ but lower than the values obtained from the PFY-XAS due to the neglected $4f^0$ component.

C. Temperature and pressure dependences

The temperature dependence of the PFY-XAS spectra for $CePd_2Si_2$ and $CeRh_2Si_2$ is shown in Fig. 4. These results show almost no temperature dependence of the electronic structures of either compound down to 8 K, within the experimental errors. This is consistent with previous XAS results obtained at the Ce M-edge down to 20 K for $CeRh_2Si_2$ and $CeRu_2Si_2$.[17] We observed a similar phenomenon for $CeIrSi_3$, in which the CEF is expected to play an important role.[22] The first excitation level of the CEF is approximately 214 K for $CePd_2Si_2$ and 350 K for $CeRh_2Si_2$, which are much higher than the respective Kondo temperatures of 10 K, and 33 or ~100 K (see Table I). The SIAM predicts changes in the electronic structure below T_K; in Ce compounds, the change corresponds to an increase of the $4f^0$ intensity.[24] Except for the temperature range where the CEF is larger than T_K, the number of f electrons is less sensitive to temperature perturbations.[25] The XAS measurements at the Ce M edge showed a $4f^0$ intensity contribution of about 1.2% for $CePd_2Si_2$ and 2.2% for $CeRh_2Si_2$ at low temperature, which suggests a higher v_R for $CeRh_2Si_2$.[17] The difference between two compounds is on the order of 1%, which is on par with the uncertainty on our estimate of v_R. Still, in Fig. 4(c), v_R is found to be constantly higher for $CeRh_2Si_2$ compared with $CePd_2Si_2$ throughout the temperature range of the measurement, which is consistent with the Ce M-edge results.

We have also measured the PFY-XAS spectra as a function of pressure at 19 K. Results, given in Fig. 5(a), show that the pressure dependence of the f^2 component is limited, while the pressure effects are very significant in the f^1 and f^0 components. This indicates that the final-state effect related the f^2 component remains almost unchanged with pressure, while increased hybridization affects the f^1 and f^0 components. Estimates of the pressure dependence of v_R as obtained from the fits of the PFY-XAS spectra are shown in Fig. 5(b). In Fig. 5(c) the pressure dependence of the Néel temperature and the superconducting transition temperature are also shown.[7] The v_R value constantly increases with pressure, it changes especially rapidly above ~5 GPa, which exceeds the pressure range of the superconductivity dome.
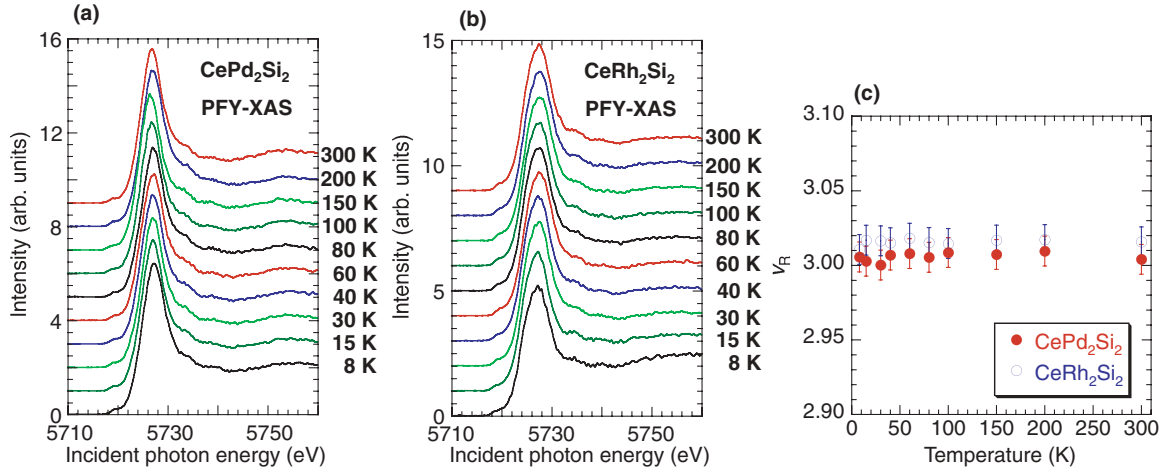
FIG. 4. (Color online) Temperature dependence of the PFY-XAS spectra for (a) CePd$_2$Si$_2$ and (b) CeRh$_2$Si$_2$. Temperature dependence of the Ce valence (closed circles) derived from the PFY-XAS spectra is shown in (c) for CePd$_2$Si$_2$ (closed circles) and CeRh$_2$Si$_2$ (open circles). v_R is the spectral weight ratio related to the Ce valence in the final state (see text for details).

We note that the lowest temperature in this study is significantly higher than T_c due to technical limitations related to cooling a membrane-driven high-pressure cell with a cryostat. However, critical behaviors are expected to extend far beyond the critical point and signs of valence fluctuations should be observable at $T > T_c$. Furthermore, our result indicates that the Ce valence is nearly insensitive to the temperature down to 8 K. We therefore consider that it is relevant to discuss the correlation between the pressure dependence of the valence as we measured it at 19 K and the occurrence of superconductivity.

The relationship of the physical properties among CeCu$_2$Si$_2$, CePd$_2$Si$_2$, and CeRh$_2$Si$_2$ has been discussed previously.[26] CePd$_2$Si$_2$ is a localized antiferromagnet, CeRh$_2$Si$_2$ an itinerant ferromagnet, and CeCu$_2$Si$_2$ is categorized as a heavy fermion with higher T_K than others. In Ce compounds, applied pressure increases the Kondo temperature and the c-f hybridization, resulting in increased intensity of the f^0 component. Our high-pressure measurements demon-

strate the pressure-induced changes in the electronic structures of CePd$_2$Si$_2$ from the localized $4f$ state to the hybridized itinerant state. These pressure-induced changes are compared with theoretical calculations in the Discussion.

IV. DISCUSSION

We have derived the valence v_R which includes the final-state effect from the experimental spectra [Fig. 5(b)]. Here we discuss the relation between the valence number v_R estimated from the PFY-XAS spectra and the number in the ground state (v_g), as well as their dependences on the hybridization strength, corresponding to the pressure, using calculations based on the SIAM. The final-state interaction causes some differences between the v_g and the v_R in Ce compounds.[22] In the present calculations, the temperature was a fixed parameter at 0 K to compare the calculated results with the experimental ones at low temperatures, 8 and 19 K. We considered the SIAM[27–30] consisting of the Ce $4f$ and conduction band
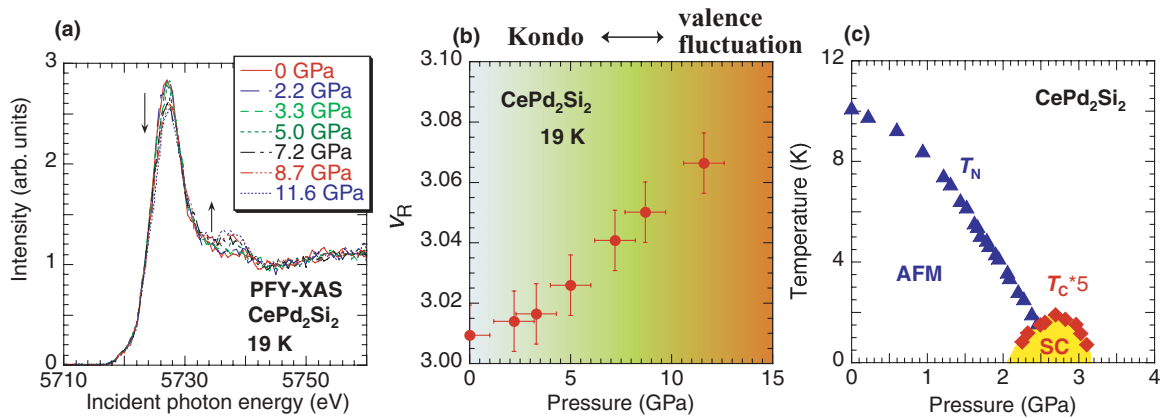

FIG. 5. (Color online) (a) Pressure dependence of the PFY-XAS spectra at 19 K for CePd$_2$Si$_2$. Arrows indicate the spectral sequence with increasing pressure. (b) Pressure dependence of the Ce valence derived from the PFY-XAS spectra. v_R is the spectral weight ratio defined in the text, corresponding to the Ce valence including final state effect. (c) Pressure dependence of the Néel temperature (T_N) and superconducting transition temperature (T_C). The data are taken from the literature.[7]

states mixed with the hybridization V. We assumed that the conduction band is half-filled and its density of states (DOS) is of rectangular shape with a width W. For simplicity we only took into account the $4f$ states with the total angular momentum $J = 5/2$. The energy of this $4f$ level is presented as ϵ_f. The Coulomb interaction between the $4f$ electrons is denoted as U_{ff}. We considered two cases: infinitely large U_{ff} and $U_{ff} = 4.5$ eV. We calculated T_K, v_g, and v_R as a function of V in the lowest order approximation in the $1/N_f$ expansion method[27] (degeneracy $N_f = 2J + 1 = 6$ for Ce).[22,31] We took $W = 4.0$ eV and $\epsilon_f = -0.8$ eV, where ϵ_f is measured from the Fermi level.

In order to calculate the v_R values, we calculated the PFY-XAS spectra as a narrowed version of the conventional L_3 XAS spectra, in which the core-hole potential acting on the $4f$ states $U_{fc} = 11.5$ eV, and the Ce $5d$ DOS of semielliptic shape with width 6 eV were considered. We did not explicitly take the atomic multiplet-coupling effect into account due to the multipole Coulomb interaction, which can cause somewhat the broadening of the PFY-XAS spectra.[29] For our parameter values of the SIAM, we started from standard ones for the mixed valence Ce compounds, but then adjusted them, to some extent, in order to reproduce better the experimental data for CePd$_2$Si$_2$. We considered the effect of the core-hole potential on the hybridization V, which makes V in the final state smaller when compared to the initial state. This effect was taken into account by multiplying V by a factor of 0.6, which reasonably describes a small fraction of the $4f^2$ component observed experimentally.

In Fig. 6 we show the calculated PFY-XAS spectra for $V = 0.263$ eV and $V = 0.35$ eV with corresponding experimental results, respectively, at 0 and 11.6 GPa, as derived from the fits to the PFY-XAS spectra in Fig. 4(a). We took into account the
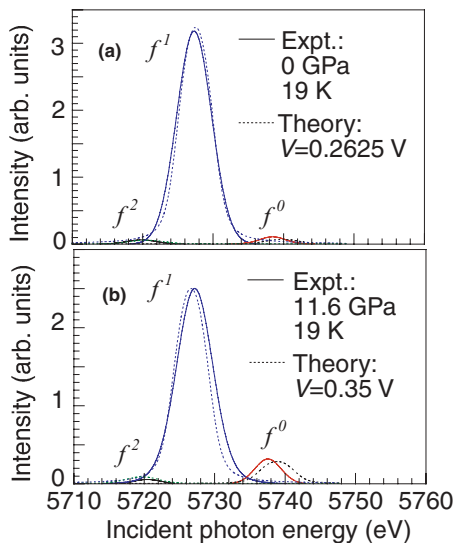
spectral broadening due to the total experimental resolution (full width at half maximum) of 2.0 eV (Gaussian width) and 1.5 eV (Lorentzian width due to core-hole lifetime broadening) for the emitted photons. Additional spectral broadening due to the multiplet coupling effect is included in these spectral widths.[29]

Figure 7 shows the calculated valence number, T_K, and the fraction of the f^n states as a function of V. In CePd$_2$Si$_2$ T_K is about 10 K,[16] corresponding to $V \simeq 0.263$ eV from
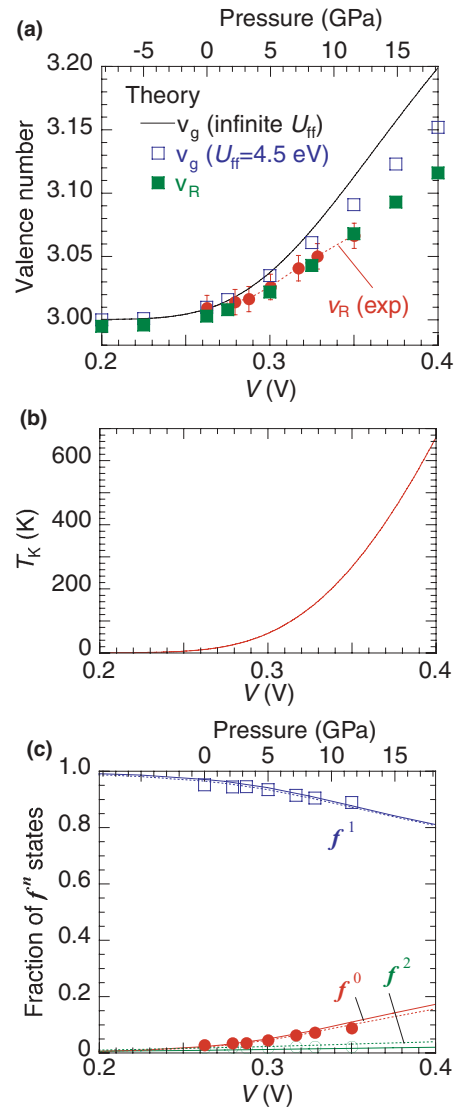
FIG. 7. (Color online) Comparison of the experimental results for CePd$_2$Si$_2$ with theory. (a) Valence number as a function of V (lower horizontal axis) and pressure (upper horizontal axis). Closed circles are experimental results. Solid line, open square, and closed square correspond to the valences calculated theoretically for the ground state with infinite U_{ff}, the ground state with $U_{ff} = 4.5$ V, and final state, respectively. (b) Theoretically calculated Kondo temperature (T_K) as a function of V. (c) Theoretical fraction of f^n states shown as a function of V (lower horizontal axis) and pressure (upper horizontal axis). Solid and dashed lines are theoretical weight for the ground and final states, respectively. Intensities of f^0 (closed circles), f^1 (open square), and f^2 (open circle) components are obtained from the fits of the experimental PFY-XAS spectra.

FIG. 6. (Color online) Intensity of f^0, f^1, and f^2 components as a function of incident photon energy for CePd$_2$Si$_2$. Solid and dashed lines correspond to the result obtained from the fit to the experimental PFY-XAS spectrum subtracting the arctanlike background and theoretical calculation, respectively. (a) Experiment: 0 GPa at 19 K. Theory: $V = 0.2625$ V. (b) Experiment: 11.6 GPa at 19 K. Theory: $V = 0.35$ V.

Fig. 7(b). In Fig. 7(a) we adjust the pressure range so that the experimental v_R agrees well with the theoretical v_R; the maximum pressure of the experiment at 11.6 GPa corresponds to $V \simeq 0.35$ V. In this treatment, we consider that the pressure-dependence of V plays the most important role for the pressure-dependence of v_g and v_R. The effect of the pressure-dependence of ϵ_f and W is assumed to be effectively included in that of V. Based on the mostly linear relation between V and pressure, these theoretical results reproduce their experimental counterparts. Our calculations indicate that the difference between v_R and v_g is larger as pressure or V increases. From Fig. 7(b), T_K of CePd$_2$Si$_2$ at 10 GPa is around 200 K.

In Fig. 7(c) we compare the theoretical and experimental fractions of the f^n states as a function of V. Again, a good agreement between theory and experiment is observed. These results show that the fraction of the f^1 component is almost the same in the initial and final states, while the fractions of the f^0 and f^2 components slightly increases and decreases, respectively, in going from the initial state to the final state, causing the difference between v_g and v_R. We also find that the fraction of the f^2 component is insensitive to the pressure increase. Both theoretical and experimental results for CePd$_2$Si$_2$ concur with the general trend in compressed Ce systems,[22,32,33] showing that the hybridization and T_K, and accordingly the valence number, all continuously increase with pressure.

We note that two values of T_K have been previously reported for CeRh$_2$Si$_2$ as ~ 100 K using NMR,[8] and 33 K based on quasielastic neutron scattering.[34] Here we find that the electronic structures of CePd$_2$Si$_2$ and CeRh$_2$Si$_2$ at ambient pressure are nearly identical, suggesting a very close T_K for both compounds. Based on the results summarized in Fig. 6 for CePd$_2$Si$_2$, $T_K = 33$ K corresponds to $V \simeq 0.286$ eV and $v_R \simeq 3.01$, and $T_K = 100$ K does 0.315 eV and $v_R \simeq 3.03$. We can therefore conclude that $T_K = 100$ K is unlikely for CeRh$_2$Si$_2$.

The application of pressure on Ce systems usually induces a decrease of f DOS at the Fermi level (E_F), of the magnetic moment, and therefore of γ.[35,36] Note that γ is written as $\gamma = \frac{C_V}{T} = \frac{1}{3}\pi^2 k_B^2 N(E_F)$, where C_V, k_B, and $N(E_F)$ are the specific heat, the Boltzmann constant, and the DOS at E_F, respectively. As shown in Figs. 5(b) and 7(a) in Ce systems under pressure, an increase of the hybridization strength usually induces a transition from the Kondo or heavy fermion regime to a valence fluctuation regime.[22] This trend is, of course, consistent with the decrease of γ. Seemingly CePd$_2$Si$_2$ is tuned to valence fluctuation regime above 10 GPa by pressure, although the boundary between them is ambiguous. In the pressure range where superconductivity occurs, the change in the Ce valence is small, and does not seem to affect superconductivity directly, which is consistent with the scenario of the magnetically mediated superconductivity in

CePd$_2$Si$_2$.[7] The rapid increase of the Ce valence above the superconducting regime in CePd$_2$Si$_2$ resembles that of other Ce superconductors such as CeIrSi$_3$[23] and CeFeAsO$_{1-y}$.[32] This may suggest negative effect of the strong valence fluctuation on the superconductivity.

Finally, we note that an increase in pressure in CePd$_2$Si$_2$ was reported to induce a change in thermopower from negative to positive around 1 GPa, which could be a signature of the two-channel Kondo effect.[15] If there is two-channel Kondo effect, one may expect to find an anomaly in the pressure dependence of the valence as in TmTe.[37] No anomaly was detected in the pressure dependence of CePd$_2$Si$_2$ within our experimental accuracy, which could be due to the fact that the valence increase is very small within the pressure range corresponding to the thermopower crossover.

V. CONCLUSION

CePd$_2$Si$_2$ and CeRh$_2$Si$_2$ are observed to exhibit weak valence fluctuations, constituting mainly Ce^{3+} (f^1) with a small fraction of Ce^{4+} (f^0). No temperature dependence of the electronic structure for either compound is observed within the experimental uncertainties at temperatures as low as 8 K. This behavior may be understood by considering the crystal electric field effect within the SAIM. The measured pressure dependence of the Ce valence in CePd$_2$Si$_2$ at 19 K showed that the Ce valence increases constantly with pressure. Theoretical calculations based on the SAIM reproduce the experimental results well. Above ~ 5 GPa, the Ce valence changes rapidly, indicating the transition from the Kondo regime into the valence fluctuation regime. Theoretical calculations indicate that the difference between v_g and v_R is larger with increasing pressure, especially in the valence fluctuation regime. This finding may be applied to understand compressed Ce systems in general. The change in the Ce valence seems not to have an effect on the occurrence of superconductivity directly, supporting the scenario of the magnetically mediated superconductivity in CePd$_2$Si$_2$.

[1] O. Stockert, S. Kirchner, F. Steglich, and Q. Si, J. Phys. Soc. Jpn. **81**, 011001 (2012).

[2] T. Endstra, G. J. Nieuwenhuys, and J. A. Mydosh, Phys. Rev. B **48**, 9595 (1993).

[3] M. Matsumoto, M. J. Han, J. Otsuki, and S. Y. Savrasov, Phys. Rev. Lett. **103**, 096403 (2009).

[4] F. M. Grosche, S. R. Julian, N. D. Mathur, and G. G. Lonzarich, Physica B **223-224**, 50 (1996).

[5] R. Movshovich, T. Graf, D. Mandrus, J. D. Thompson, J. L. Smith, and Z. Fisk, Phys. Rev. B **53**, 8241 (1996).

[6] S. Araki, M. Nakashima, R. Settai, T. C. Kobayashi, and Y. Ōnuki, J. Phys.: Codens. Matter **14**, L377 (2002).

[7] N. D. Mathur, F. M. Grosche, S. R. Julian, I. R. Walker, D. M. Freye, R. K. Haselwimmer, and G. G. Lonzarich, Nature (London) **394**, 39 (1998).

[8] Y. Kawasaki, K. Ishida, Y. Kitaoka, and K. Asayama, Phys. Rev. B **58**, 8634 (1998).

[9] I. Sheikin, Y. Wang, F. Bouquet, P. Lejay, and A. Junod, J. Phys.: Codens. Matter **14**, L543 (2002).

[10] S. Raymond, D. Jaccard, H. Wilhelm, and R. Cerny, Solid State Commun. **112**, 617 (1999).

[11] S. Kawarazaki, M. Sato, Y. Miyako, N. Chigusa, K. Watanabe, N. Metoki, Y. Koike, and M. Nishi, Phys. Rev. B **61**, 4167 (2000).

[12] V. Vildosola, A. M. Llois, and J. G. Sereni, Phys. Rev. B **69**, 125116 (2004).

[13] V. Vildosola, A. M. Llois, and M. Alouani, Phys. Rev. B **71**, 184420 (2005).

[14] H. Abe, H. Kitazawa, H. Suzuki, G. Kido, and T. Matsumoto, J. Magn. Magn. Mater. **177-181**, 479 (1998).

[15] P. Link, D. Jaccard, and P. Lejay, Physica B **225**, 207 (1996).

[16] A. Severing, E. Holland-Moritz, B. D. Rainford, S. R. Culverhouse, and B. Frick, Phys. Rev. B **39**, 2557 (1989).

[17] T. Willers, D. T. Adroja, B. D. Rainford, Z. Hu, N. Hollmann, P. O. Körner, Y.-Y. Chin, D. Schmitz, H. H. Hsieh, H.-J. Lin, C. T. Chen, E. D. Bauer, J. L. Sarrao, K. J. McClellan, D. Byler, C. Geibel, F. Steglich, H. Aoki, P. Lejay, A. Tanaka, L. H. Tjeng, and A. Severing, Phys. Rev. B **85**, 035117 (2012).

[18] E. Settai, A. Misawa, S. Araki, M. Kosaki, K. Suguyama, T. Takeuchi, K. Kindo, Y. Haga, E. Yamamoto, and Y. Ōnuki, J. Phys. Soc. Jpn. **66**, 2260 (1997).

[19] H. Yamaoka, I. Jarrige, N. Tsujii, J.-F. Lin, T. Ikeno, Y. Isikawa, K. Nishimura, R. Higashinaka, H. Sato, N. Hiraoka, H. Ishii, and K.-D. Tsuei, Phys. Rev. Lett. **107**, 177203 (2011).

[20] Y. Feng, R. Jaramillo, J. Wang, Y. Ren, and T. F. Rosenbaum, Rev. Sci. Instrum. **81**, 041301 (2010).

[21] H. Yamaoka, Y. Zekko, I. Jarrige, J.-F. Lin, N. Hiraoka, H. Ishii, K.-D. Tsuei, and J. Mizuki, J. Appl. Phys. **112**, 124503 (2012).

[22] H. Yamaoka, A. Kotani, Y. Kubozono, A. M. Vlaicu, H. Oohashi, T. Tochio, Y. Ito, and H. Yoshikawa, J. Phys. Soc. Jpn. **80**, 014702 (2011).

[23] H. Yamaoka, I. Jarrige, N. Tsujii, A. Kotani, J.-F. Lin, F. Honda, R. Settai, Y. Ōnuki, N. Hiraoka, H. Ishii, and K.-D. Tsuei, J. Phys. Soc. Jpn. **80**, 124701 (2011).

[24] N. E. Bickers, D. L. Cox, and J. W. Wilkins, Phys. Rev. B **36**, 2036 (1987).

[25] P. Bonville, J. A. Hodges, P. Imbert, D. Jaccard, J. Sierro, M. J. Besnus, and A. Meyer, Physica B **163**, 347 (1990).

[26] P. Pedrazzini, M. Gómez Berisso, O. Trovarelli, J. G. Sereni, and C. Geibel, J. Low Temp. Phys. **135**, 143 (2004).

[27] O. Gunnarsson and K. Schönhammer, Phys. Rev. B **28**, 4315 (1983).

[28] A. Kotani, T. Jo, and J. C. Parlebas, Adv. Phys. **37**, 37 (1988).

[29] A. Kotani and H. Ogasawara, J. Electron. Spectrosc. Relat. Phenom. **60**, 257 (1992).

[30] F. de Groot and A. Kotani, *Core Level Spectroscopy of Solids* (CRC, Boca Raton, FL/Taylor & Francis, London, 2008).

[31] A. Kotani, Eur. Phys. J. B **72**, 375 (2009).

[32] H. Yamaoka, I. Jarrige, A. Ikeda-Ohno, S. Tsutsui, J.-F. Lin, N. Takeshita, K. Miyazawa, A. Iyo, H. Kito, H. Eisaki, N. Hiraoka, H. Ishii, and K.-D. Tsuei, Phys. Rev. B **82**, 125123 (2010).

[33] J.-P. Rueff, S. Raymond, M. Taguchi, M. Sikora, J.-P. Itié, F. Baudelet, D. Braithwaite, G. Knebel, and D. Jaccard, Phys. Rev. Lett. **106**, 186405 (2011).

[34] T. Graf, J. D. Thompson, M. F. Hundley, R. Movshovich, Z. Fisk, D. Mandrus, R. A. Fisher, and N. E. Phillips, Phys. Rev. Lett. **78**, 3769 (1997).

[35] M. Ilkhani, M. R. Abolhassani, and M. Aslaninejad, Eur. Phys. J. B **65**, 21 (2008).

[36] P. Gegenwart, Q. Si, and F. Steglich, Nature Phys. **4**, 186 (2008).

[37] I. Jarrige, J.-P. Rueff, S. R. Shieh, M. Taguchi, Y. Ohishi, T. Matsumura, C.-P. Wang, H. Ishii, N. Hiraoka, and Y. Q. Cai, Phys. Rev. Lett. **101**, 127401 (2008).